

1 **The impact of non-pharmaceutical interventions on the prevention** 2 **and control of COVID-19 in New York City**

3 Jiannan Yang¹, Qingpeng Zhang¹, Zhidong Cao^{2,3,4}, Jianxi Gao⁵, Dirk Pfeiffer⁶, Lu Zhong⁷, Daniel Dajun
4 Zeng^{2,3,4}

5

6 1. School of Data Science, City University of Hong Kong, Hong Kong, China.

7 2. The State Key Laboratory of Management and Control for Complex Systems, Institute of Automation,
8 Chinese Academy of Sciences, Beijing, China.

9 3. School of Artificial Intelligence, University of Chinese Academy of Sciences, Beijing, China.

10 4. Shenzhen Artificial Intelligence and Data Science Institute (Longhua), Shenzhen, China.

11 5. Department of Computer Science, Rensselaer Polytechnic Institute, Troy, NY, USA.

12 6. Department of Infectious Diseases and Public Health, City University of Hong Kong, Hong Kong,
13 China.

14 7. Department of Mechanical, Aerospace, and Nuclear Engineering, Rensselaer Polytechnic Institute,
15 Troy, NY, USA.

16

17 Correspondence to: Qingpeng Zhang (qingpeng.zhang@cityu.edu.hk), Daniel Dajun Zeng

18 (dajun.zeng@ia.ac.cn)

19

20 **Abstract**

21 The emergence of coronavirus disease 2019 (COVID-19) has infected more than 37 million people
22 worldwide. The control responses varied across countries with different outcomes in terms of epidemic
23 size and social disruption. In this study, we presented an age-specific susceptible-exposed-infected-
24 recovery-death model that considers the unique characteristics of COVID-19 to examine the effectiveness
25 of various non-pharmaceutical interventions (NPIs) in New York City (NYC). Numerical experiments
26 from our model show that the control policies implemented in NYC reduced the number of infections by
27 72% (IQR 53-95), and the number of deceased cases by 76% (IQR 58-96) by the end of 2020,
28 respectively. Among all the NPIs, social distancing for the entire population and the protection for the
29 elderly in the public facilities is the most effective control measure in reducing severe infections and
30 deceased cases. School closure policy may not work as effectively as one might expect in terms of
31 reducing the number of deceased cases. Our simulation results provide novel insights into the city-
32 specific implementation of NPIs with minimal social disruption considering the locations and population
33 characteristics.

34 **Keywords**

35 SARS-CoV-2, mathematical model, non-pharmaceutical interventions

36 **Introduction**

37 The outbreak of coronavirus disease 2019 (COVID-19) has become a global pandemic with unanticipated
38 consequences to the global community. As of 13 October 2020, severe acute syndrome coronavirus 2
39 (SARS-CoV-2), the cause of COVID-19, has infected more than 37 million people and resulted in more
40 than 1 million deaths (1). A variety of non-pharmaceutical interventions (NPIs) were introduced to reduce
41 the transmission by lowering contact intensity at different locations (2), such as school closure, workplace
42 shutdown, and the closure of bars, churches, and other public facilities, which has been shown to be
43 successful in China (3), South Korea (4), and other countries (5). The NPIs, such as city-wide school
44 closures, were implemented as part of its State of Emergency plan (6) in New York City (NYC) that has
45 been identified as a major epicenter with over 258,000 cases and 23,915 confirmed deaths (7). However,
46 the effectiveness of these NPIs remains unclear, promoting a critical need to evaluate them and to derive
47 more effective NPIs with the consideration of social disruption.

48
49 Increasing evidence shows that the demographic structure and age-specific contacts at different locations
50 play an essential role in the COVID-19 epidemic, as well as the effectiveness of varying NPIs (8-12). For
51 instance, school closure is useful in controlling the infections among the young people (13, 14), who tend

52 to have mild or moderate symptoms and usually can recover without treatment. On the other hand, severe
53 and deceased cases are often among the elderly and those with comorbidities (15). According to the data
54 from the CDC of the US, 79.2% of death in the US are the population whose age is over 64. (16) Existing
55 studies (17, 18) addressed this problem by dividing the population into several age groups and defining
56 the social contacts at different locations. However, utilizing these unique epidemiological characteristics
57 to reduce the total number of infections and the severe and deceased cases and the social disruption is
58 under-researched.

59

60 In this article, we develop a novel age-specific susceptible-exposed-infected-recovery-death (A-SEIRD)
61 model (19, 20) to examine the effect of a set of common NPIs on reducing the total number of infections
62 and the severe and deceased cases. More importantly, we obtain the NPIs that can contain the epidemic
63 with minimal social disruption by quantitatively examining all possible NPIs. The latest epidemiological
64 parameters (21, 22) of COVID-19 were adopted by the A-SEIRD model.

65

66 Methods

67 Adjusted Contact Matrix and Transmission Rate

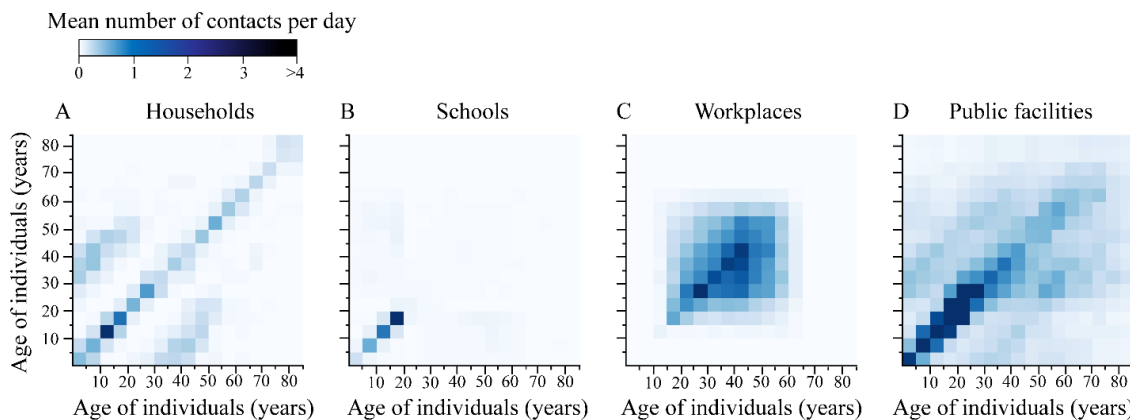
68 The contact patterns vary across locations. Previous studies (17, 18) divide the contact intensity into four
 69 locations within a city: households, workplaces, schools, and public facilities represented as C^H , C^W , C^S ,
 70 and C^P individually. Note here the original contact matrix C is estimated by survey data achieved in 2008
 71 (17). To get the updated contact matrix, we adjust the original contact matrix C by the latest population
 72 structure that refers to the age distribution which is assumed to be static during the simulation period for
 73 the same city. We divide the total population of a city into 17 age groups including 16 groups with a 5-
 74 year band between birth and 80-year-old, and the 17th group representing aged >80. The adjusted contact
 75 intensity (M_{ij}) of age group j made by age group i is obtained by taking the product of C_{ij} and the ratio of
 76 the current population sizes of age group i (p_i) and age group j (p_j) as follows:

$$77 \quad M_{ij} = C_{ij} \times \frac{p_i}{p_j}, \quad (1)$$

78 The overall social mixing pattern is defined as the weighted sum of the adjusted contact matrix across the
 79 four locations,

$$80 \quad M = w^H M^H + w^W M^W + w^S M^S + w^P M^P, \quad (2)$$

81 where w^H , w^W , w^S , w^P are the location-specific decay factors compared to the normal situation ($w^H =$
 82 $w^W = w^S = w^P = 1$) and the effects of different NPIs are reflected by the reduction of these decay
 83 factors. The contact matrixes of the four locations under the normal situation are shown in Figure 1.
 84



85
 86 **Figure 1: Age-specific and location-specific contact intensities under normal situation for NYC.**

87 (A), (B), (C), and (D) denote the contact intensity among all the 17 age groups, respectively. The grid in
 88 each panel represents the mean number of contact per day. The colour change denotes the value change:
 89 more blue, more contacts.

90

91 The transmission rate β varies with NPIs shown on the overall adjusted social mixing pattern M .
 92 Following Prem et al. (17) we projected the adjusted contact matrix with the basic reproduction number to
 93 the transmission rate as follows:

$$94 \quad \det(M - \lambda I) = 0, \quad (3)$$

$$95 \quad \beta = \frac{R_0}{\max(\lambda) \times d_I}, \quad (4)$$

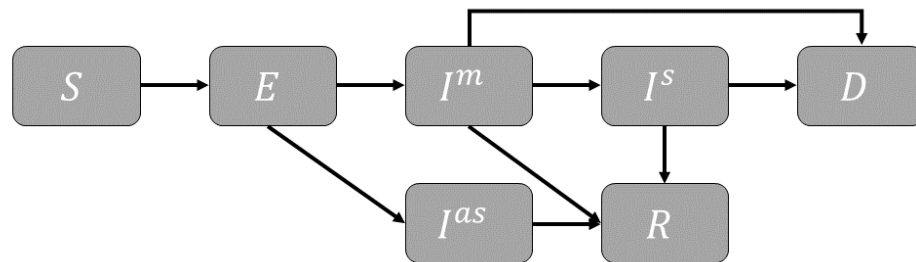
96 where R_0 is the basic reproduction number and d_I is the average length of the infectious period.

97

98 **The A-SEIRD Model**

99 The proposed A-SEIRD model is based on the classic SEIR model (19, 20). In the classic SEIR model,
 100 the population is divided into four groups according to the infection status: susceptible (S), exposed (E),
 101 infected (I), and recovery (E). Based on the evidence of the asymptomatic infections of COVID-19 (23,
 102 24), we add three new statuses for the infected individuals: asymptotically infected (I^{as}), mildly
 103 infected (I^m) and severely infected (I^s). Susceptible individuals may become exposed after contacting
 104 infected ones. Exposed individuals may become either mildly infected or asymptotically infected. We
 105 assume that the deceased cases come from both mild and severe infections, and all asymptotically
 106 infected individuals will recover. The model structure is presented in Figure 2.

107



108

109 **Figure. 2: The proposed age-specific SEIRD model.**

110

111 Considering the huge drop in human movement between cities (25), we assume that NYC is a closed
 112 system throughout the course of the epidemic (from 1 Jan 2020 to 31 Dec 2020) and initially there are
 113 1,000 infected individuals for simplicity. The initially infected individuals are distributed in different age
 114 groups with the same proportion (0.016%). The epidemic parameters are age-dependent, such as the elder
 115 individuals have a higher severe rate and death rate than the youth (22).

116 For a given age group i , the epidemic transitions can be described by

$$117 \quad \frac{dS_i}{dt} = - \sum_{j=1}^n \beta M_{ij} \frac{I_j^m}{N_j} S_i - \sum_{j=1}^n \alpha \beta M_{ij} \frac{I_j^{as}}{N_j} S_i, \quad (5)$$

$$118 \quad \frac{dE_i}{dt} = \sum_{j=1}^n \beta M_{ij} \frac{I_j^m}{N_j} S_i + \sum_{j=1}^n \alpha \beta M_{ij} \frac{I_j^{as}}{N_j} S_i - \sigma_i E_i, \quad (6)$$

$$119 \quad \frac{dI_i^{as}}{dt} = \rho_i \cdot \sigma_i E_i - \gamma_i^{as} I_i^{as}, \quad (7)$$

$$120 \quad \frac{dI_i^m}{dt} = (1 - \rho_i) \sigma_i E_i - \gamma_i^m (1 - \mu_i - \kappa_i^m) I_i^m - \mu_i I_i^m - \kappa_i^m I_i^m, \quad (8)$$

$$121 \quad \frac{dI_i^s}{dt} = \mu_i I_i^m - \gamma_i^s \cdot (1 - \kappa_i^s) I_i^s - \kappa_i^s I_i^s, \quad (9)$$

$$122 \quad \frac{dR_i}{dt} = \gamma_i^{as} I_i^{as} + \gamma_i^m (1 - \mu_i - \kappa_i^m) I_i^m + \gamma_i^s \cdot (1 - \kappa_i^s) I_i^s, \quad (10)$$

$$123 \quad \frac{dD_i}{dt} = \kappa_i^m I_i^m + \kappa_i^s I_i^s, \quad (11)$$

124 where S_i , E_i , I_i^{as} , I_i^m , I_i^s , R_i , and D_i denote the number of susceptible, latent, asymptomatic infectious,
 125 mild infectious, severe infectious, recovery, and deceased individuals at age group i , respectively. N_j is
 126 the number of individuals in age group j . β is the transmission rate that differs by the contact intensity
 127 and population structure and α is the proportion of the transmission rate of the asymptomatic infections
 128 over that of the mild infections (26). Note that here we assume the severe infections will not spread the
 129 virus due to their limited mobility (usually isolated in hospital). M_{ij} denotes the total contact intensity of
 130 age group j made by age group i . For individuals in the age group i , $\rho_i = I_i^{as} / (I_i^{as} + I_i^m)$ is the estimated
 131 fraction of asymptomatic cases among both asymptomatic and mild infections; $\sigma_i = 1/d_L$ is the daily
 132 probability that an exposed individual becomes infectious (either asymptomatic or mild) where d_L is the
 133 average latent period; γ_i^{as} , γ_i^m , and γ_i^s are the daily recovery probability for the asymptomatic, mild, and
 134 severe infections, respectively. They are related to specific disease period: $\gamma_i^{as} = 1/d_l$, $\gamma_i^m = 1/d_m$,
 135 $\gamma_i^s = 1/d_s$, where d_l , d_m , d_s are the infectious period, mild duration, and severe duration generated from
 136 literature, respectively. μ_i is the daily probability of hospitalisation that a mildly infected patient becomes
 137 severely infected. $\kappa_i^m = \kappa_i^s = \psi_i/d_d$ is the daily crude mortality rate, where ψ_i is the crude mortality rate
 138 and d_d is the period from the symptom onset to death. The crude mortality rate ψ_i is estimated from the
 139 official confirmed case report (27) which equals the proportion of the number of deceased individuals to
 140 the infected individuals within one age group. The parameters used in the model from literature are
 141 presented in Table 1 and Table 2.

142

143 **Table 1. The parameters used in the model from the literature.**

Parameters	Value	Reference
------------	-------	-----------

Basic reproduction number R_0	2.0 (1.3-2.6)*	Riou and Althaus (21)
Mean latent (incubation) period d_L	6.0 days	Li et al.(28)
Mean infectious period d_I	4.6 days	Moghadas et al. (29)
The proportion of the transmission rate of the asymptomatic infections over that of the mild infections α	1.0 for all ages	Assumption
The fraction of asymptomatic cases among both asymptomatic and mild infections ρ_i	0.4 for all ages	Nishiura et al. (30)
Mild duration d_m	10 days for all age groups	Wang et al. (31)
Severe duration d_s	16.25 days for all ages	Moghadas et al. (29)
The period from symptom onset to death d_d	10 days for all ages	Yang et al. (32)

144 *Data are median (IQR).

145

146 **Table 2. The age-specific parameters used in the model from the literature.**

Description	0-19	19-44	45-65	65-75	75+	Reference
Daily probability of hospitalisation μ	0.0250	0.0320	0.0320	0.6400	0.6400	Moghadas et al. (29) and WHO-China Joint Mission Report (33)
Crude mortality rate ψ	0.0215	0.0782	0.2257	0.4600	0.6085	Estimated from official confirmed case report (27)

147

148 **Non-Pharmaceutical Intervention Scenarios**

149 Some study (34) points out that the seeding of the virus likely occurred in the US between 25 December
150 2019 and 15 January 2020, thus we set the starting date of the simulation to be 1 January 2020 for a better
151 fitting, and simulate the epidemic based on the real-time responses by the government. Before the state
152 governor declared a state of emergency in New York State on 7 March, we assume the residents have
153 already had a certain degree of awareness of the COVID-19, and thus the contact intensities at schools,
154 workplaces, and public facilities were reduced by 20%. Between the emergency declaration and the state-
155 wide stay-at-home order (7 March to 22 March), the awareness of precaution has been elevated to reduce
156 the contact intensity at workplaces, schools, and public facilities by 50%. After the state-at-home order
157 was put in place, the city was at a full lockdown status (6), so we set the decay factor of the contact
158 intensity at schools to 0 and further reduce the contact intensities at workplaces and the public facilities to
159 30% of the normal situation. To model the four reopening phases (35) implemented on 8 June, 22 June, 6
160 July, and 20 July, respectively, we assume the contact intensities at both the workplaces and public
161 facilities increase by 5% at each phase. In addition, we simulate the scenario in which NYC has a larger-
162 scale reopen back to the situation before the state-at-home order (50% for all locations except household)
163 on 1 September. The decay factor of contacts in households is set to 1 over the course of the epidemic.

164
165 We investigate five common NPIs: theoretical no intervention, school closure, social distancing for the
166 entire population, social distancing for the elderly (age > 64 years) (36), and adaptive policy proposed by
167 Ferguson et al. (37). In the adaptive policy, a stringent control measure (full lockdown) is triggered when
168 certain conditions are met. Here we assume that the condition is the number of daily new severely
169 infected cases is over N . We examined two values of N (100 and 150) for the robustness of results. The
170 details of the decay factor setting for each NPIs are shown in Table 3. We assume the NPIs were
171 implemented through the whole course of the epidemic simulation.

172

173 **Table 3. Summary of NPIs considered.**

NPIs	Description
Theoretical no intervention	$M = M^H + M^W + M^S + M^P$
School closure	$M = M^H + M^W + 0 \times M^S + M^P$
Social distancing for the entire population	$M = M^H + 0.5M^W + 0.5M^S + 0.5M^P$
The social distancing for the elderly (age > 64 years)	$M = M^H + w^E M^W + w^E M^S + w^E M^P$ $w^E = \begin{bmatrix} 1 & 0 & 0 & \dots & 0 & 0 & 0 \\ 0 & 1 & 0 & \dots & 0 & 0 & 0 \\ 0 & 0 & \vdots & \dots & \vdots & 0 & 0 \\ 0 & 0 & 0 & \dots & 0 & \vdots & 0 \\ 0 & 0 & 0 & \dots & 0.5 & 0 & \vdots \\ \vdots & \vdots & \vdots & \dots & 0 & 0.5 & 0 \\ 0 & 0 & 0 & \dots & 0 & 0 & 0.5 \end{bmatrix}$
Adaptive policy	$M = M^H + 0 \times M^W + 0 \times M^S + 0.1M^P$ <i>if</i> $N_s > 100$ (150) where N_s denotes the number of new severe infections per day

174

175 **Identifying Effective NPIs Considering Social Disruption**

176 The objective of NPIs should not be limited to reducing infections without the consideration of social
 177 disruption. First, we measure the social disruption caused by the NPIs at the four locations. Here, the
 178 social disruption at a location is measured as $(1 - w)M \times s$, which is the product of the reduced amount
 179 of contacts $(1 - w)M$ and the relative importance of these contacts s . Thus, the total social disruption L
 180 caused by the NPIs can be represented as follows,

$$181 \quad L = s^S(1 - w^S)M^S + s^H(1 - w^H)M^H + s^W(1 - w^W)M^W + s^P(1 - w^P)M^P. \quad (12)$$

182

183 Second, we aim to identify the NPIs that reduce the social disruption L as much as possible under the
 184 condition that the COVID-19 epidemic does not exceed that of the actual NPIs implemented in NYC.
 185 Specifically, we consider three measures of the COVID-19 epidemic: the number of all infections, the
 186 number of severe infections, and the number of deceased cases as of 31 December 2020, respectively.

187 It is challenging to quantify the relative importance of the activities at different locations in a very
188 detailed manner. In this study, we make the following intuitive assumptions about relative importance:
189 workplaces have the highest importance, $s^W = 1$; public facilities has the second highest importance,
190 $s^P = 0.5$; households and schools have the lowest importance, $s^H = s^S = 0.2$. Here, we set low
191 importance for school thanks to the availability of online schooling. We also consider the simplified
192 scenario in which the relative importance of all locations is identical. Therefore, in total, we consider
193 three distinct measures of the COVID-19 epidemic and two assumptions about the relative importance of
194 locations, so in total, we consider six scenarios, as illustrated by Table 4.

195
196 For intuitive interpretation and simple implementation, we discretize the continuous value of the decay
197 factors into 11 discrete values with equal intervals, 0, 0.1, 0.2, ..., 0.9, 1.0. We set the minimal decay
198 factor of the contacts at the public facilities to 0.1 as it is unrealistic to shut down all public facilities. In
199 addition, we assume that $w^H = 1$, because there is little we can do for the contacts within households. In
200 this way, the total number of solutions is restricted to $11 \times 11 \times 10 \times 1 = 1210$ for each of the six
201 scenarios, and an exhaustive search can be used to identify the best NPIs for a certain scenario.

202

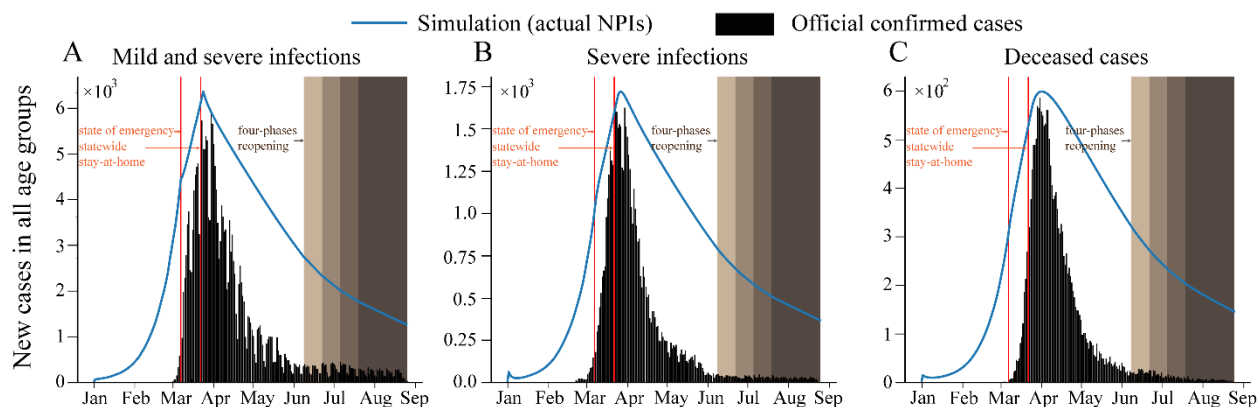
203

204 Results

205 Fit the Model from Data

206 Figure 3 presents the comparison of the simulation results of the proposed A-SEIRD model and the
207 number of confirmed cases in NYC (27). Note that the simulation of the A-SEIRD model obtains the
208 onset of COVID-19. The actual confirmation of COVID-19 infection usually has a six-days-delay (38).
209 Thus, we incorporated the six-days-delay in presenting the simulation results in Figure 3. In general, the
210 simulation results (blue curve) capture the trend of the confirmed case data (black bars). The simulated
211 curve is higher than the confirmed curve, which is common given the wide existence of undiagnosed
212 cases (39). The implementations of the control measures are represented by the red lines, and the four-
213 phases reopening policies are represented by the brown bars. The effects of control measures became
214 obvious with a lag of several weeks, due to the incubation period of the disease. Additionally, the
215 reopening slowed down the decreasing trend.

216



217

218 **Figure. 3: Comparison of our simulation results with the official confirmed case report.**

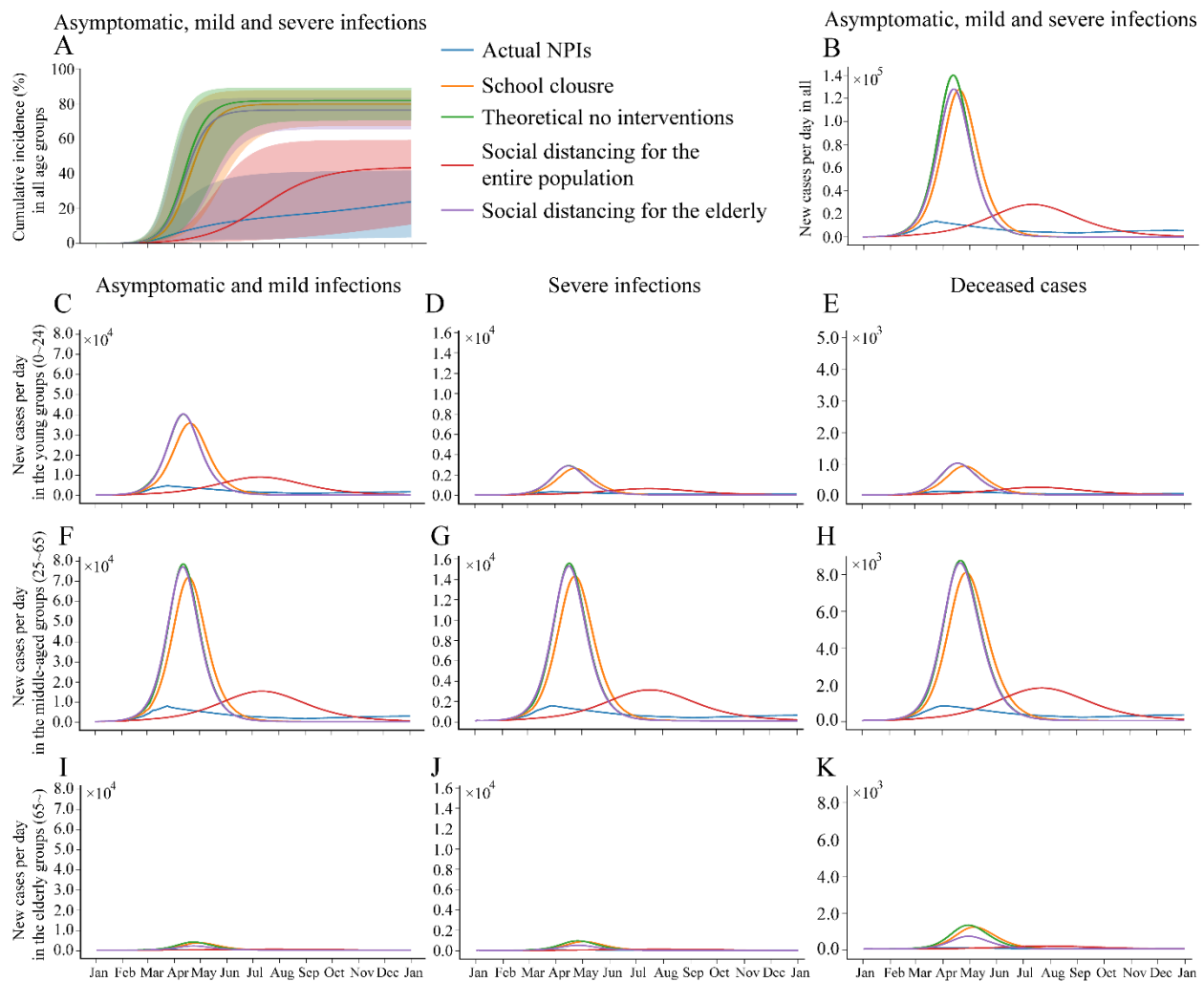
219 (A) The number of new mild and severe infections. (B) The number of new severe infections. (C) The
220 number of new deceased cases. The blue curve and black bars represent the simulated results and the
221 confirmed cases, respectively. The red vertical lines and brown bars indicate the control measures and
222 four reopening phases put in place in NYC.

223

224 Quantify the Effectiveness of NPIs

225 We present the simulated epidemic sizes with the five common NPIs in Figure 4. Without any control, we
226 would expect a peak of asymptomatic and mild infections in early April. The peak of severe infections
227 occurs two-week later due to disease progression. In such a case, 70% (IQR 60-77) of NYC residents
228 would be infected by the end of 2020. The peak of deceased cases is around early May. Comparing the
229 case with actual NPIs and theoretical no intervention scenario, we observe a 72% (IQR 53-95) decline in

230 the total number of infections and a 76% (IQR 58-96) decline in the number of deceased cases. The
 231 effects of each NPIs vary across age categories. More specifically, school closure is effective: the total
 232 infections and deceased cases are nearly the same as the results of those without any control (theoretical
 233 no intervention). School closure slightly reduces (4% (IQR 3-7)) the number of infections among young
 234 people (< 25 years), who are not the most vulnerable. On the other hand, the social distancing for the
 235 entire population effectively reduces 47% (IQR 33-84) of infections and 51% (IQR 39-86) deceased
 236 cases. In addition, social distancing for the elderly could reduce 47% (IQR 46-56) of total infections and
 237 47% (IQR 46-48) deceased cases in the elderly groups (> 64 years), but not so much for other age groups.



238

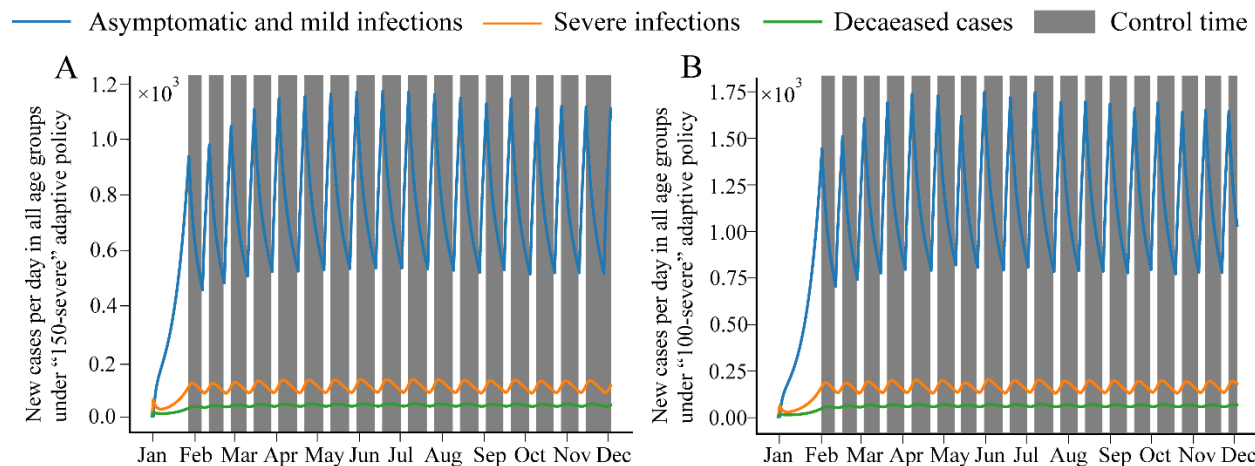
239 **Figure 4: The effects of different NPIs on cumulative cases and new cases per day among age**
 240 **groups.**

241 The effects of different NPIs on the cumulative incidence and the number of new cases per day for all are
 242 presented in **A** and **B**, respectively. The shaded areas around the coloured lines in panel **A** represent the

243 IQR. The effects of different NPIs on the number of new cases per day for three age groups: the young
244 groups who aged <25 years (**C**, **D**, and **E**), the middle-aged groups who aged 25 to 64 years (**F**, **G**, and
245 **H**), the elderly groups who aged > 64 years (**I**, **J**, and **K**).

246
247 We also examined the effectiveness of the adaptive policy, which naturally forms an oscillation curve as
248 shown in Figure 5. The grey blocks represent the periods with stringent strategies (“full lockdown”). We
249 adopt two variants of the adaptive policy from Ferguson et al. (37), “100-severe” (with 100 new severe
250 infections per day as the threshold to trigger the control), and “150-severe” (with 150 as the threshold).
251 Results show that both adaptive policies can reduce the total number of infections and the number of
252 severe infections well. However, the triggered time period of the control is too long, and the interval is
253 only around six days. In practice, such frequent switches between different policies are not realistic.

254



255

256 **Figure 5: Effects of the two adaptive policies.**

257 (A) “150-severe” adaptive policy. (B) “100-severe” adaptive policy. The blue, orange, and green lines
258 denote the number of new cases per day at all age groups considering the number of asymptomatic, mild,
259 severe infections and deceased cases, respectively. The grey blocks represent the periods with suppression
260 strategies (“full lockdown”).

261

262 Identify the Best NPIs

263 We derive the best NPIs by exhaustively examining all the possible 1210 solutions for each of the six
264 scenarios introduced in Methods. All scenarios lead to similar NPIs: to reduce the contact intensity at
265 public facilities (social distancing for the entire population) while largely maintaining the function of
266 schools and workplaces. This indicates that, although school closure is associated with lower social

267 disruption, the model still prefers to sacrifice the contact at public facilities because it is associated with
 268 higher risk by mixing various age groups in the city.
 269

270 **Table 4. Effective NPIs for each of the six scenarios.**

Scenario	Social function score weights	Status	Results
TOI	$s^S = s^H = s^W = s^P = 1$	$I^{as} + I^m + I^s$	$M = M^H + 0.8M^W + M^S + 0.1M^P$
SOI	$s^S = s^H = s^W = s^P = 1$	I^s	$M = M^H + 0.8M^W + M^S + 0.1M^P$
DOI	$s^S = s^H = s^W = s^P = 1$	D	$M = M^H + 0.7M^W + M^S + 0.1M^P$
TOA	$s^S = s^H = 0.2, s^P = 0.5, s^W = 1$	$I^{as} + I^m + I^s$	$M = M^H + 0.8M^W + M^S + 0.1M^P$
SOA	$s^S = s^H = 0.2, s^P = 0.5, s^W = 1$	I^s	$M = M^H + 0.8M^W + 0.9M^S + 0.1M^P$
DOA	$s^S = s^H = 0.2, s^P = 0.5, s^W = 1$	D	$M = M^H + 0.8M^W + M^S + 0.1M^P$

271 TOI, SOI, DOI stands for identity relative importance of the activities at different locations under three
 272 measures of the COVID-19 epidemic: the number of all infections, severe infections, and deceased cases
 273 individually. TOA, SOA, DOA stands for intuitive assumptions of the relative importance of the contacts
 274 at different locations under three measures of the COVID-19 epidemic: the number of all infections,
 275 severe infections, and deceased cases individually.
 276

277 **Discussion**

278 Since most COVID-19 infections appear to have mild or moderate symptoms that can heal themselves
279 and there are many asymptomatic cases (15), it is critical to reduce the number of severely infected and
280 deceased cases rather than only flattening the total epidemic curve. In this study, we expanded the age-
281 specific SEIR model to develop a new A-SEIRD model that considers the asymptomatic infections of
282 COVID-19 and evaluated the effectiveness of various NPIs in NYC. We found that not all the NPIs were
283 effective, and the social distancing at the public facilities are essential for reducing the number of severe
284 infections and deaths.

285
286 Counterintuitively, we find that nearly all the countries decided to close the schools, while our model
287 shows that it is not that effective in controlling the epidemic. As shown in Figure 4, school closure would
288 only slightly reduce the number of total infections compared to the extreme theoretical no intervention
289 policy. As shown in Figure 1. It is obvious that the contacts in schools concentrated on the young
290 population (age <25 years) who make up only a small fraction of the vulnerable population. Meanwhile,
291 the contacts among the young population are also very active in households and public facilities. Thus,
292 school closure alone may not work as effectively as one would have expected. A recent systematic review
293 (40) also concluded that there are no data on the relative contribution of school closures to transmission
294 control and some modelling studies proved that school closure would prevent only 2-4% deceased cases
295 (37). At the same time, school closure would bring more pressure on the medical system since many
296 healthcare workers would be distracted to take care of their children. Jude et al.'s modelling analysis
297 found that 28.8% (95% CI 28.5–29.1) of the health-care workforce need to provide care for children aged
298 3–12 years (14). A trade-off needs to be taken into consideration while making the school closure
299 decision.

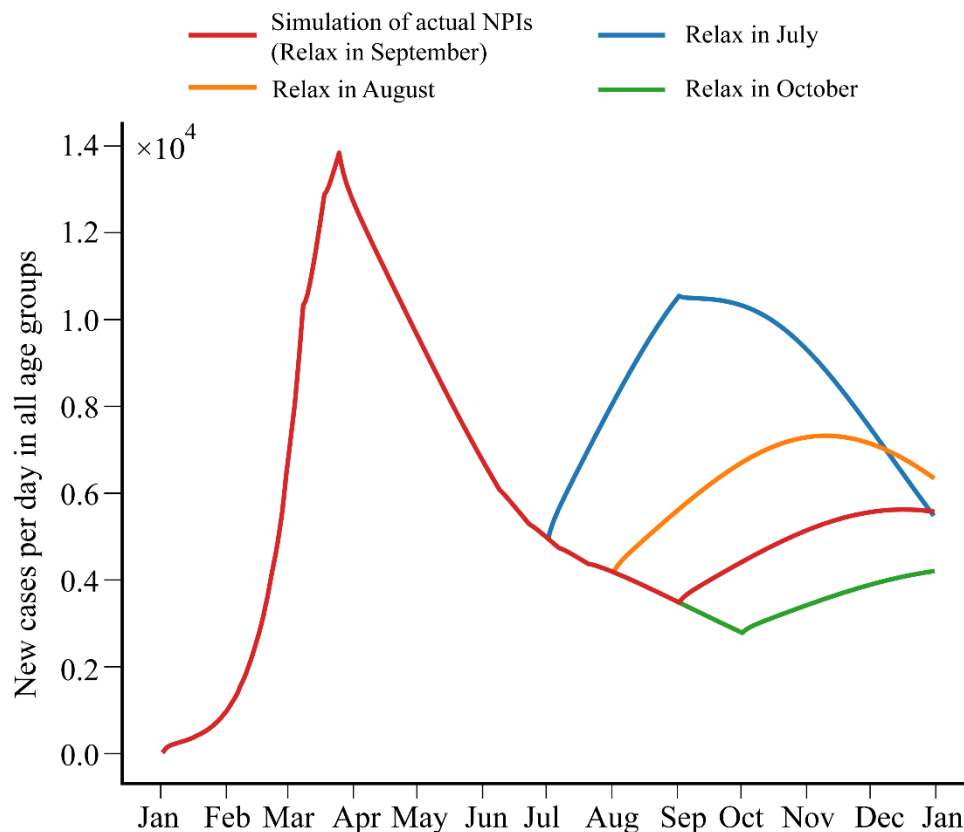
300
301 Compared with the social distancing only for the elderly, social distancing for the entire population comes
302 with greater social disruption. Thunström et al. (41) found that the cost of social distancing measures is
303 \$7.21 trillion in the USA utilized epidemiological and economic forecasting. Although the social
304 distancing for the elderly would not significantly reduce the total number of infections, it can effectively
305 reduce the number of deceased cases. These results reflect the clinical characteristics of COVID-19: high
306 transmissibility but a high mortality rate only among the elderly (42, 43). That is why the social
307 distancing for the elderly policy has already been adopted in many countries (44).

308
309 NPIs lead to social disruptions. We used the proposed A-SEIRD model to identify the NPIs that flatten
310 the curve with minimal social disruptions. We found that the social distancing at public facilities could

311 effectively reduce the number of infections and the number of deaths. As shown in Figure 1, the contacts
312 of the elderly are concentrated in public facilities and households. Although it is difficult to shut down all
313 the public facilities, we suggest that the social distancing for the elderly only at the public facilities would
314 be an effective and practical way to reduce the number of deceased cases without large-scale social
315 disruption. In practice, the protection of the elderly in public areas has already been adopted, such as
316 cresting flow to make room for the elderly in the supermarket.

317
318 Apparently, it is not practical to implement the NPIs for a long period, because the social disruption could
319 lead to enormous economic loss, which may, in turn, cause other public health problems. Here, we
320 simulated the ongoing process when relaxing at the beginning of July, August, September, and October as
321 shown in Figure 6. Our model suggests that relaxation after the peak of the outbreak would cause an
322 instant rebound. At the same time, it can be observed that the later relaxing implemented, the smaller the
323 rebound size is. Thus, the resumption of work and production shall be carefully taken place. The adaptive
324 policy, which seems to work in controlling the epidemic size, but leads to unrealistically frequent
325 switches between lockdown and relaxation, making it difficult to be realized (Figure 5).

326



327

328 **Fig. 6: The impacts of policy relaxations in July, August, September, and October.**

329 The lines denote the number of new cases. The colours of the lines represent the results of different
330 policies: the simulation of actual NPIs (relax in September) (red), relax in July (blue), August (orange),
331 and October (green).

332

333 In conclusion, our study proposed a comprehensive mathematical model that takes into account both the
334 age-specific contacts between people, the latest epidemiological parameters of the COVID-19, and the
335 social disruption. The simulation results provide novel insights into the implementation of NPIs with
336 minimal social disruption. We call for more research on the trade-off between epidemic control and
337 economic loss.

338 **Code Availability**

339 The source codes have been made available on Github: [https://github.com/JasonJYang/Age-specific-](https://github.com/JasonJYang/Age-specific-SEIRD)
340 [SEIRD](https://github.com/JasonJYang/Age-specific-SEIRD).

341 **Funding**

342 This work was supported in part by grants from the National Natural Science Foundation of China
343 (72042018).

344 **References**

- 345 1. WHO. Coronavirus disease 2019 (COVID-19): Weekly Epidemiological Update.
346 <https://www.who.int/publications/m/item/weekly-epidemiological-update---24-november-2020>.
347 Accessed November 30, 2020. 2020.
- 348 2. Anderson RM, Heesterbeek H, Klinkenberg D, Hollingsworth TD. How will country-
349 based mitigation measures influence the course of the COVID-19 epidemic? *The Lancet*.
350 2020;395(10228):931-4.
- 351 3. Chen S, Yang J, Yang W, Wang C, Bärnighausen T. COVID-19 control in China during
352 mass population movements at New Year. *The Lancet*. 2020;395(10226):764-6.
- 353 4. Shim E, Tariq A, Choi W, Lee Y, Chowell G. Transmission potential and severity of
354 COVID-19 in South Korea. *Int J Infect Dis*. 2020;93:339-44.
- 355 5. Cheng VCC, Wong SC, Chen JHK, Yip CCY, Chuang VWM, Tsang OTY, et al.
356 Escalating infection control response to the rapidly evolving epidemiology of the coronavirus
357 disease 2019 (COVID-19) due to SARS-CoV-2 in Hong Kong. *Infect Control Hosp Epidemiol*.
358 2020;41(5):493-8.
- 359 6. Cuomo GAM. Governor Cuomo Signs the 'New York State on PAUSE' Executive Order.
360 [https://www.governor.ny.gov/news/governor-cuomo-signs-new-york-state-pause-executive-](https://www.governor.ny.gov/news/governor-cuomo-signs-new-york-state-pause-executive-order)
361 [order](https://www.governor.ny.gov/news/governor-cuomo-signs-new-york-state-pause-executive-order). Accessed August 11, 2020. 2020.
- 362 7. Health. NYSDo. COVID-19 tracker. [https://covid19tracker.health.ny.gov/views/NYS-](https://covid19tracker.health.ny.gov/views/NYS-COVID19-Tracker/NYSDOHCOVID-19Tracker-Map?%3Aembed=yes&%3Atoolbar=no&%3Atabs=n)
363 [COVID19-Tracker/NYSDOHCOVID-19Tracker-](https://covid19tracker.health.ny.gov/views/NYS-COVID19-Tracker/NYSDOHCOVID-19Tracker-Map?%3Aembed=yes&%3Atoolbar=no&%3Atabs=n)
364 [Map?%3Aembed=yes&%3Atoolbar=no&%3Atabs=n](https://covid19tracker.health.ny.gov/views/NYS-COVID19-Tracker/NYSDOHCOVID-19Tracker-Map?%3Aembed=yes&%3Atoolbar=no&%3Atabs=n). Accessed November 30, 2020. 2020.
- 365 8. Prem K, Liu Y, Russell TW, Kucharski AJ, Eggo RM, Davies N, et al. The effect of
366 control strategies to reduce social mixing on outcomes of the COVID-19 epidemic in Wuhan,
367 China: a modelling study. *The Lancet Public Health*. 2020.
- 368 9. Davies NG, Klepac P, Liu Y, Prem K, Jit M, Eggo RM. Age-dependent effects in the
369 transmission and control of COVID-19 epidemics. Preprint at
370 <https://www.medrxiv.org/content/10.1101/2020.03.24.20043018v2>. medRxiv.
371 2020:2020.03.24.20043018.
- 372 10. Yin H, Liu Z, Kammen DM. Impacts of Early Interventions on the Age-Specific
373 Incidence of COVID-19 in New York, Los Angeles, Daegu and Nairobi. Preprint at
374 <https://www.medrxiv.org/content/10.1101/2020.04.19.20071803v1>. medRxiv.
375 2020:2020.04.19.20071803.
- 376 11. Liu Y, Gu Z, Xia S, Shi B, Zhou X-N, Shi Y, et al. What are the Underlying
377 Transmission Patterns of COVID-19 Outbreak?—An Age-specific Social Contact
378 Characterization. *EClinicalMedicine*. 2020:100354.

- 379 12. Santesmasses D, Castro JP, Zenin AA, Shindyapina AV, Gerashchenko MV, Zhang B, et
380 al. COVID-19 is an emergent disease of aging. Preprint at
381 <https://www.medrxiv.org/content/10.1101/2020.04.15.20060095v1>. medRxiv.
382 2020:2020.04.15.20060095.
- 383 13. Earn DJ, He D, Loeb MB, Fonseca K, Lee BE, Dushoff J. Effects of school closure on
384 incidence of pandemic influenza in Alberta, Canada. *Annals of internal medicine*.
385 2012;156(3):173-81.
- 386 14. Bayham J, Fenichel EP. Impact of school closures for COVID-19 on the US health-care
387 workforce and net mortality: a modelling study. *The Lancet Public Health*. 2020;5(5):e271-e8.
- 388 15. Epidemiology Working Group for NCIP Epidemic Response CCfDC, Prevention. The
389 epidemiological characteristics of an outbreak of 2019 novel coronavirus diseases (COVID-19)
390 in China. *Chinese Journal of Epidemiology*. 2020;41(02):145-51.
- 391 16. CDC-USA. CDC COVID Data Tracker. [https://covid.cdc.gov/covid-data-](https://covid.cdc.gov/covid-data-tracker/#demographics)
392 [tracker/#demographics](https://covid.cdc.gov/covid-data-tracker/#demographics). Accessed November 30, 2020. 2020.
- 393 17. Prem K, Cook AR, Jit M. Projecting social contact matrices in 152 countries using
394 contact surveys and demographic data. *PLoS Comput Biol*. 2017;13(9):e1005697.
- 395 18. Fumanelli L, Ajelli M, Manfredi P, Vespignani A, Merler S. Inferring the structure of
396 social contacts from demographic data in the analysis of infectious diseases spread. *PLoS*
397 *Comput Biol*. 2012;8(9):e1002673.
- 398 19. Klepac P, Caswell H. The stage-structured epidemic: linking disease and demography
399 with a multi-state matrix approach model. *Theoretical Ecology*. 2011;4(3):301-19.
- 400 20. Wu JT, Leung K, Leung GM. Nowcasting and forecasting the potential domestic and
401 international spread of the 2019-nCoV outbreak originating in Wuhan, China: a modelling study.
402 *The Lancet*. 2020.
- 403 21. Riou J, Althaus CL. Pattern of early human-to-human transmission of Wuhan 2019 novel
404 coronavirus (2019-nCoV), December 2019 to January 2020. *Eurosurveillance*.
405 2020;25(4):2000058.
- 406 22. Verity R, Okell LC, Dorigatti I, Winskill P, Whittaker C, Imai N, et al. Estimates of the
407 severity of coronavirus disease 2019: a model-based analysis. *The Lancet Infectious Diseases*.
408 2020.
- 409 23. Mizumoto K, Kagaya K, Zarebski A, Chowell G. Estimating the asymptomatic
410 proportion of coronavirus disease 2019 (COVID-19) cases on board the Diamond Princess cruise
411 ship, Yokohama, Japan, 2020. *Eurosurveillance*. 2020;25(10):2000180.
- 412 24. Day M. Covid-19: four fifths of cases are asymptomatic, China figures indicate. *British*
413 *Medical Journal Publishing Group*; 2020.
- 414 25. Badr HS, Du H, Marshall M, Dong E, Squire MM, Gardner LM. Association between
415 mobility patterns and COVID-19 transmission in the USA: a mathematical modelling study. *The*
416 *Lancet Infectious Diseases*. 2020.
- 417 26. Liu Y, null n, Funk S, Flasche S. The contribution of pre-symptomatic infection to the
418 transmission dynamics of COVID-2019 [version 1; peer review: 1 approved]. *Wellcome Open*
419 *Research*. 2020;5(58).
- 420 27. NYC-Government. COVID-19: Data. [https://www1.nyc.gov/site/doh/covid/covid-19-](https://www1.nyc.gov/site/doh/covid/covid-19-data.page)
421 [data.page](https://www1.nyc.gov/site/doh/covid/covid-19-data.page). Accessed November 30, 2020. 2020.
- 422 28. Li Q, Guan X, Wu P, Wang X, Zhou L, Tong Y, et al. Early Transmission Dynamics in
423 Wuhan, China, of Novel Coronavirus–Infected Pneumonia. *New England Journal of Medicine*.
424 2020;382(13):1199-207.

- 425 29. Moghadas SM, Shoukat A, Fitzpatrick MC, Wells CR, Sah P, Pandey A, et al. Projecting
426 hospital utilization during the COVID-19 outbreaks in the United States. *Proc Natl Acad Sci U S*
427 *A*. 2020;117(16):9122-6.
- 428 30. Nishiura H, Kobayashi T, Miyama T, Suzuki A, Jung S, Hayashi K, et al. Estimation of
429 the asymptomatic ratio of novel coronavirus infections (COVID-19). Preprint at
430 <https://www.medrxiv.org/content/10.1101/2020.02.03.20020248v2>. medRxiv.
431 2020:2020.02.03.20020248.
- 432 31. Wang D, Hu B, Hu C, Zhu F, Liu X, Zhang J, et al. Clinical Characteristics of 138
433 Hospitalized Patients With 2019 Novel Coronavirus–Infected Pneumonia in Wuhan, China.
434 *JAMA*. 2020;323(11):1061-9.
- 435 32. Yang X, Yu Y, Xu J, Shu H, Liu H, Wu Y, et al. Clinical course and outcomes of
436 critically ill patients with SARS-CoV-2 pneumonia in Wuhan, China: a single-centered,
437 retrospective, observational study. *The Lancet Respiratory Medicine*. 2020.
- 438 33. CHINA W. WHO&China. Report of the WHO-China Joint Mission on Coronavirus
439 Disease 2019 (COVID-19). 2020.
- 440 34. Du Z, Javan E, Nugent C, Cowling BJ, Meyers LA. Using the COVID-19 to influenza
441 ratio to estimate early pandemic spread in Wuhan, China and Seattle, US. *EClinicalMedicine*.
442 2020:100479.
- 443 35. Stevens MGM. "What Are the Phases of New York's Reopening Plan?"
444 <https://www.nytimes.com/article/new-york-phase-reopening.html>. Accessed September 4, 2020.
445 *The New York Times* 2020.
- 446 36. WHO. "WHO | Definition of an older or elderly person".
447 <https://www.who.int/healthinfo/survey/ageingdefnolder/en/>. Accessed September 4, 2020. 2011.
- 448 37. Ferguson N, Laydon D, Nedjati Gilani G, Imai N, Ainslie K, Baguelin M, et al. Report 9:
449 Impact of non-pharmaceutical interventions (NPIs) to reduce COVID19 mortality and healthcare
450 demand. 2020.
- 451 38. Bi Q, Wu Y, Mei S, Ye C, Zou X, Zhang Z, et al. Epidemiology and transmission of
452 COVID-19 in 391 cases and 1286 of their close contacts in Shenzhen, China: a retrospective
453 cohort study. *The Lancet Infectious Diseases*. 2020;20(8):911-9.
- 454 39. Holmdahl I, Buckee C. Wrong but useful—what covid-19 epidemiologic models can and
455 cannot tell us. *New England Journal of Medicine*. 2020.
- 456 40. Viner RM, Russell SJ, Croker H, Packer J, Ward J, Stansfield C, et al. School closure and
457 management practices during coronavirus outbreaks including COVID-19: a rapid systematic
458 review. *The Lancet Child & Adolescent Health*. 2020;4(5):397-404.
- 459 41. Thunström L, Newbold SC, Finnoff D, Ashworth M, Shogren JF. The Benefits and Costs
460 of Using Social Distancing to Flatten the Curve for COVID-19. *Journal of Benefit-Cost*
461 *Analysis*. 2020;11(2):179-95.
- 462 42. Novel CPERE. The epidemiological characteristics of an outbreak of 2019 novel
463 coronavirus diseases (COVID-19) in China. *Zhonghua liu xing bing xue za zhi= Zhonghua*
464 *liuxingbingxue zazhi*. 2020;41(2):145.
- 465 43. Huang C, Wang Y, Li X, Ren L, Zhao J, Hu Y, et al. Clinical features of patients infected
466 with 2019 novel coronavirus in Wuhan, China. *The lancet*. 2020;395(10223):497-506.
- 467 44. BBC. Coronavirus: isolation for over-70s 'within weeks'.
468 <https://www.bbc.co.uk/news/uk-51895873>. Accessed August 8, 2020. 2020.

469